

Corrosion of CVD Silicon Carbide in 500°C Supercritical Water

E. Barringer,[†] Z. Faiztompkins, and H. Feinroth

Ceramic Tubular Products, Rockville, Maryland 20855

T. Allen

Department of Engineering Physics, University of Wisconsin, Madison, Wisconsin 53706

M. Lance, H. Meyer, L. Walker, and E. Lara-Curzio

Oak Ridge National Laboratory, Oak Ridge, Tennessee 37831

A high-purity CVD β -SiC showed a relatively low corrosion rate in deoxygenated supercritical water at 500°C. The corrosion rate was lower than that previously reported for CVD SiC in 360°C water and much lower than that reported for sintered and reaction-bonded SiC. The present study confirmed that CVD SiC was preferentially attacked at the grain boundaries. Analytical examinations did not reveal the presence of a measurable oxide scale. As a result, it is believed that corrosion of the high-purity SiC occurred via hydrolysis to hydrated silica species at the surface that were rapidly dissolved into the supercritical water.

I. Introduction

THE use of SiC in commercial nuclear reactors, particularly as cladding for advanced fuels, could provide substantial safety and economic benefits. Zirconium alloy cladding materials that are presently used in light water reactors present limitations in heat ratings and overall fuel burnup due to their loss of strength during reactor flow transients and during other overheating accidents, surface oxidation at high burnup, and their potential for exothermic metal water reactions at design base loss of coolant accident conditions. On the other hand, SiC possesses excellent high-temperature mechanical properties, and it has been shown to be stable under neutron irradiation.^{1,2} However, the stability of SiC in water coolants under typical LWR operating conditions must be demonstrated before this material can be deployed in commercial water reactors.

Hydrothermal corrosion of SiC has been the subject of numerous investigations.^{3–8} Of particular interest, Hirayama *et al.* found that the dissolution rate of SiC in water at 290°C is accelerated by the increase in pH value and the amount of oxygen dissolved.³ They also reported that the dissolution rate of SiC in an oxygenated alkaline solution follows linear kinetics, whereas in an acidic solution, it approximates parabolic kinetics. Microstructural analysis revealed that corrosion occurred at the grain boundaries and that there was no evidence for the formation of a protective SiO₂ layer.³

Kim *et al.*^{7,8} reported that CVD SiC exhibited better corrosion resistance than reaction-bonded SiC (RBSC) and sintered

SiC (SSC) in water at 360°C, that residual-free silicon (Si) in RBSC was preferentially corroded, and that the kinetics of corrosion followed a parabolic law, except for abrupt increases in weight loss after 7 and 10 days for SSC and CVD SiC, respectively. Kim *et al.*⁷ also showed that the corrosion of RBSC was accelerated by increasing pH through the addition of small amounts of LiOH.

Kraft *et al.*⁶ observed linear corrosion behavior for CVD SiC fibers (Specialty Materials Inc., Lowell, MA) in water at 200 MPa and temperatures in the range of 400–700°C and concluded that no protective layer had formed on the surface of the fibers.

In this study, the corrosion behavior of CVD SiC in deoxygenated supercritical water at 500°C was investigated.

II. Experimental Procedure

CVD SiC (Rohm & Hass Company, Advanced Materials, Woburn, MA) test specimens (31.75 mm × 12.7 mm × 0.38 mm) were used in this investigation (Fig. 1). The holes near the ends of each specimen were used to hold it in the test fixture. The specimens were polished to a 1 μ m RMS surface finish. The corrosion experiment was conducted at the University of Wisconsin's Supercritical Water Test Loop facility using deionized water with an average oxygen concentration of 25 parts per billion (ppb) at 500°C. Water pressure in the test loop was 25 MPa, and the flow rate over the specimens was approximately 1 m/s. Three SiC specimens were tested, one each exposed for 7, 14, and 21 days. The test also included a range of metal alloys being considered for supercritical water reactor applications, and included austenitic stainless steels, nickel-base alloys, and ferritic-martensitic steels. The specimens were weighed before and after exposure to an accuracy of 0.1 mg. After exposure, the specimens were further characterized by Raman Spectroscopy and analytical electron microscopy. Raman spectra were acquired from the surface of the samples using a Dilor XY800 Raman Microprobe (JY Inc., Edison, NJ) with a Coherent 308C Ar⁺ laser (Coherent Laser Group, Santa Clara, CA) operating at 5145 Å and 200 mW output power. Light was focused using a × 10 objective to an ~10 μ m spot size. The pH level of the water was not measured during the test. Although the pH of the water from the loop was measured after the test, the recorded values were influenced by matrix effects. As a result, pH was not considered in the interpretation of the results.

III. Results and Discussion

Figure 2 shows the weight changes for the CVD SiC coupons after exposure. Corrosion data from Kim *et al.*⁸ for CVD SiC

W.-J. Kim—contributing editor

Manuscript No. 22199. Received August 31, 2006; approved October 7, 2006.

The work at Oak Ridge National Laboratory was sponsored by the Assistant Secretary for Energy Efficiency and Renewable Energy, Office of FreedomCAR and Vehicle Technology Program, as part of the High Temperature Materials Laboratory User Program, Oak Ridge National Laboratory, managed by UT-Battelle, LLC for the U.S. Department of Energy under contract number DE-AC05-00OR22725.

[†]Author to whom correspondence should be addressed. e-mail: ebarringer@gmail.com

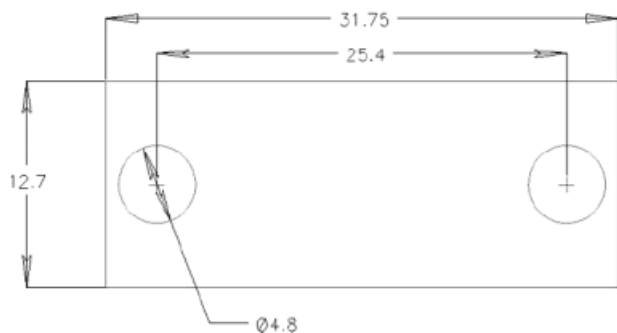


Fig. 1. SiC corrosion coupon geometry (dimensions in millimeter).

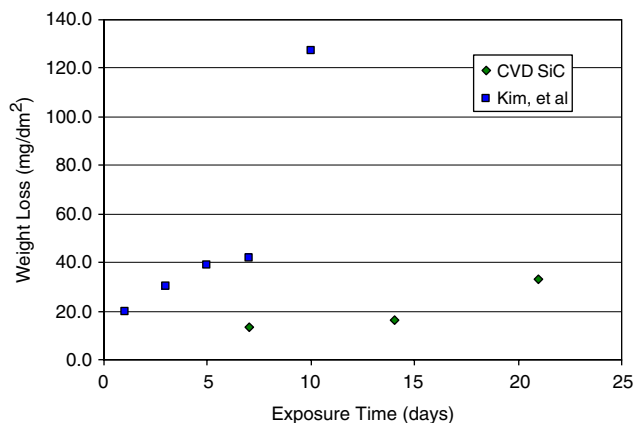


Fig. 2. Weight loss for CVD SiC after exposure to high-temperature water.

exposed to pure water at 360°C have also been included. In both cases, the weight decreased with exposure time and was significantly less than that reported for SSC⁸ or RBSC.⁷

Kim *et al.*⁸ reported that preferential corrosion had occurred along the grain boundaries, revealing large columnar grains that are typical of CVD SiC. They suggested that the preferential grain boundary corrosion was likely due to the higher energy of SiC at the grain boundaries relative to the SiC within the grains and that as the corrosion reaction proceeded, sufficient amounts of SiC were removed from the grain boundaries, resulting in the loss of grains into the water.⁸ The fall of grains into the water, as opposed to dissolution of hydrolyzed SiC, was identified as the source of the abrupt increase in weight loss after the 10-day exposure.

In the present study, the amount of weight loss was much lower than that reported by Kim *et al.* Moreover, the abrupt

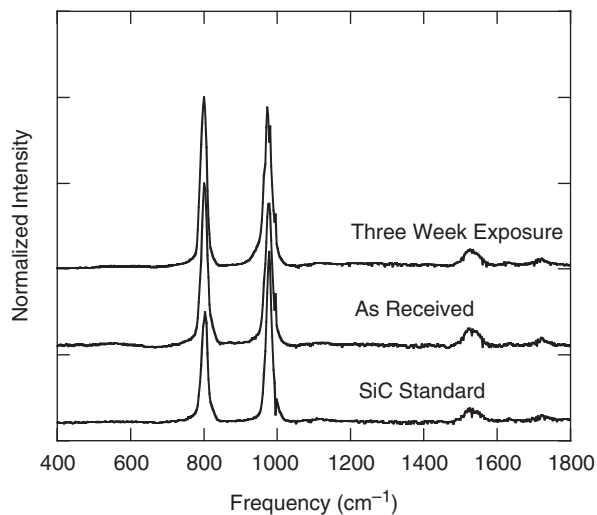


Fig. 3. Raman spectra of a stoichiometric SiC standard, the as-received CVD SiC, and the specimen surface after a 21-day exposure to 500°C water.

increase in weight loss reported by Kim *et al.* after 10 days was not seen in the present study. This result was unexpected, given that the present study used flowing water and a higher exposure temperature, which should have accelerated corrosion/erosion rates compared with exposure in stagnant water. However, the present study utilized very low oxygen levels in the water, which may have suppressed corrosion. Unfortunately, the limited number of data points precludes an accurate determination of the kinetics of corrosion. Nevertheless, in an attempt to elucidate the corrosion behavior observed in the present study, the exposed samples were characterized using analytical techniques.

Figure 3 shows Raman spectra from the surfaces of a stoichiometric SiC standard, the as-received CVD SiC, and the specimen exposed to 500°C supercritical water for 21 days. The spectrum for the standard and as-received SiC showed the expected first-order peaks at 800 and 970 cm⁻¹, and second-order peaks at 1540 and 1720 cm⁻¹. No free Si or free carbon (C) was detected for as-received CVD SiC. After 21 days of exposure, no measurable change in the Raman spectrum was observed, suggesting that preferential removal of Si or C did not occur. Moreover, no oxygen in the form of SiO₂ was detected on the surface of the specimen.

Figure 4 shows SEM micrographs of cross sections of as-fabricated CVD SiC and after exposure to supercritical water for 21 days. Evident are the large columnar grains that are typical of CVD β -SiC. After the 21-day exposure, pitting of the surface is seen at a depth of 3–5 μ m.

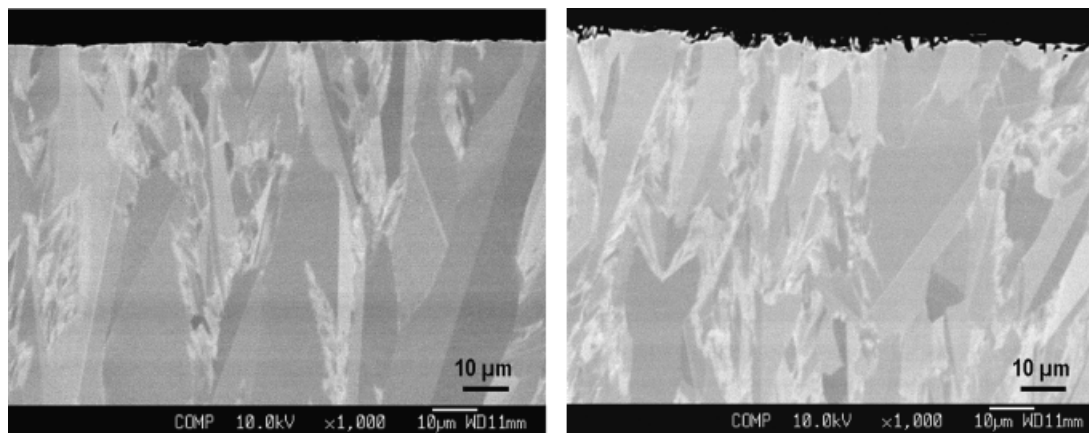


Fig. 4. SEM micrographs of fracture surfaces for as-received CVD SiC (left), and after a 21-day exposure to 500°C, 25 ppb O₂ supercritical water (right).

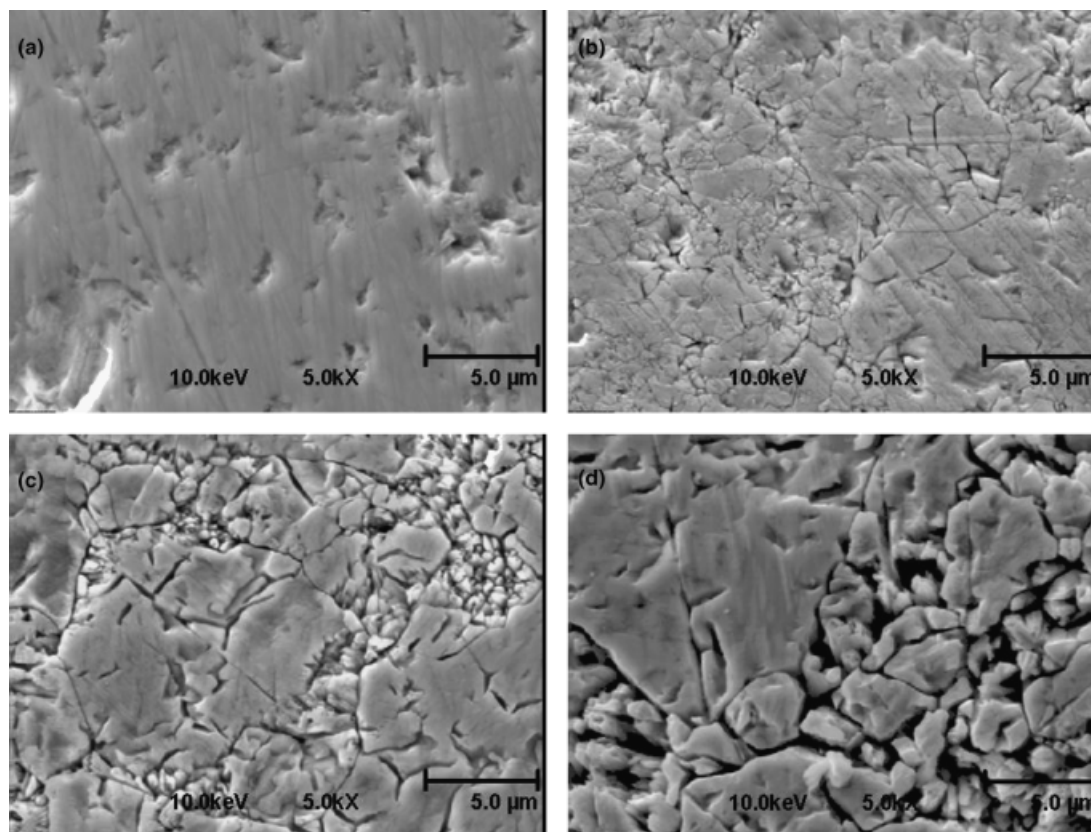


Fig. 5. SEM micrographs of surfaces for: (a) as-received CVD SiC; (b) after a 7-day exposure; (c) after a 14-day exposure; and (d) after a 21-day exposure.

Figure 5 shows the surface microstructure of the as-received CVD SiC, and after exposure to supercritical water for 7, 14, and 21 days. The surface features on the as-received sample are the result of polishing artifacts. After exposure to supercritical water, individual SiC grains can be distinguished on the surface and the amount of SiC removed clearly increases with exposure time. These images confirm that the grain boundaries are preferentially attacked, as previously reported by Kim *et al.*⁸ However, Figs. 4 and 5 show that while a small amount of SiC was removed from the grain boundaries at the surface, the depth of penetration was relatively small and there is no evidence of significant loss of surface grains.

Surface analysis by Auger spectroscopy was performed for the as-received CVD SiC and the specimens exposed to supercritical water. As shown in Table I, the surface of the as-received CVD SiC specimen contained about 48.5 at.% Si, 41.3 at.% C, and 10.2 at.% oxygen. It should be mentioned that the numbers in Table I are an average of three values from selected points representing typical surface features. For the unexposed sample, the C and Si values ranged from 35 to 38 at.% to 44 to 52 at.%, respectively. Likewise, the C/Si values for the 1-, 2-, and 3-week samples were in the range of C 48–49/Si 45–46 at.%; C 52–68/Si 28–44 at.%; and C 42–49/Si 47–54 at.%, respectively. In all cases, lower C values meant higher Si values and vice versa. The at.% of oxygen was more consistent from point to point on each sample.

Table I. Surface Composition Determined by Auger Spectroscopy (at.%)

Specimen	Silicon	Carbon	Oxygen
As-received	48.5	41.3	10.2
7 days	45.5	48.2	6.3
14 days	37.0	57.9	5.1
21 days	50.9	45.4	3.7

In general, exposure to supercritical water led to a reduction in the amount of oxygen present on the surface. The trends for Si and C tend to show a slight reduction of Si and a slight increase of C, except for the 3-week sample. This trend would be consistent with the removal of Si from the surface via hydrolysis to form Si(OH)_4 , which dissolved into water, although more data would be required to identify this mechanism positively. The composition of the surface of the specimen exposed for 21 days shows a reduction in the oxygen content, but does not follow the trend with respect to Si and C. This would indicate that a different mechanism becomes important after 14 days.

Analytical chemical analysis using an Electron Microprobe confirmed that oxygen was present only on the exposed surface, and that no measurable oxide scale was present. The results of the Auger and microprobe examinations suggest that a protective oxide (or hydrated silica) layer was not present, as has been suggested by Kim *et al.*⁸ and Hirayama *et al.*³ Rather, it is likely that SiC at the surface was hydrolyzed to form Si(OH)_4 species, which were rapidly dissolved into the flowing supercritical water. In this case, a linear relationship between weight loss and exposure time would be expected. However, insufficient data exist in the present study to confirm such a relationship.

As was shown in Fig. 1, the corrosion rate observed in the present study for CVD SiC in 500°C supercritical water was much lower than that reported by Kim *et al.*⁸ for a different CVD SiC in 360°C water. The difference in corrosion rates is not fully understood, particularly given the higher temperature and flowing water conditions used for the present study. The present study, however, was carried out with very low oxygen levels (about 25 ppb) in the water. Kim *et al.* did not specify oxygen levels for their experiment, and unless special precautions were taken, it is likely that somewhat higher oxygen levels were present (> 1 ppm). Higher oxygen concentrations in the water would lead to more rapid corrosion³ and therefore, that could explain the differences in corrosion rates. In addition, while both studies utilized high-purity CVD SiC, it appears that differences in the

microstructure, or at least orientation of the columnar grains relative to the exposed surface, existed. The columnar grains were generally oriented normal to the surface of the specimens used for the present study, while they appeared to be oriented along the surface in the SiC used by Kim *et al.*⁸ Moreover, the grains in their specimens appeared to be smaller in size. This would lead to a higher grain boundary area in their specimens, and a greater tendency to lose grains via erosion once sufficient corrosion of the grain boundaries had occurred.

IV. Summary

High-purity CVD β -SiC showed relatively low corrosion rates in deoxygenated supercritical water at 500°C. The corrosion rate was much lower than that observed for SSC and RBSC, and it was lower than that previously reported for CVD SiC in water at 360°C. The present study confirmed that CVD SiC was preferentially attacked at the grain boundaries. However, insufficient weight-loss data were collected to determine whether corrosion obeyed a linear or parabolic rate law. Analytical microscopy did not reveal the presence of a measurable oxide scale.

As a result, it is believed that corrosion occurred via hydrolysis to hydrated silica species at the surface that were rapidly dissolved into the water.

References

- ¹E. E. Bloom, "The Challenge of Developing Structural Materials for Fusion Power Systems," *J. Nuclear Mater.*, **263** [Part A] 7–17 (1998).
- ²D. J. Senor, G. E. Youngblood, C. E. Moore, D. J. Trimble, G. A. Newsome, and J. J. Woods, "Effects of Neutron Irradiation on Thermal Conductivity of SiC-Based Composites and Monolithic Ceramics," *Fusion Technol.*, **30** [3 Part 2A] 943–55 (1996).
- ³H. Hirayama, T. Kawakubo, A. Goto, and T. Kaneko, "Corrosion Behavior of Silicon Carbide in 290°C Water," *J. Am. Ceram. Soc.*, **72** [11] 2049–53 (1989).
- ⁴N. S. Jacobson, Y. G. Gogotsi, and M. Yoshimura, "Thermodynamic and Experimental Study of Carbon Formation on Carbides Under Hydrothermal Conditions," *J. Mater. Chem.*, **5**, 595–601 (1995).
- ⁵Y. Gogotsi, K. Nickel, D. Bahloul-Hourlier, T. Merie-Mejean, G. Khomenko, and K. Skjerlie, "Structure of Carbon Produced by Hydrothermal Treatment of β -SiC Powder," *J. Mater. Chem.*, **6** [4] 595–604 (1996).
- ⁶T. Kraft, K. G. Nickel, and Y. G. Gogotsi, "Hydrothermal Degradation of Chemical Vapor Deposited SiC Fibers," *J. Mater. Sci.*, **33**, 4357–63 (1998).
- ⁷W. Kim, H. Hwang, and J. Park, "Corrosion Behavior of Reaction-Bonded Silicon Carbide Ceramics in High-Temperature Water," *J. Mater. Sci. Lett.*, **21**, 733–5 (2002).
- ⁸W. Kim, H. Hwang, J. Park, and W. Ryu, "Corrosion Behavior of Sintered and Chemically Vapor Deposited Silicon Carbide Ceramics in Water at 360°C," *J. Mater. Sci. Lett.*, **22**, 581–4 (2003). □